Hollow fiber membrane contactor as a gas-liquid model contactor

Dindore, V. Y.; Brilman, D. W. F.; Versteeg, G. F.

Published in:
Chemical Engineering Science

DOI:
10.1016/j.ces.2004.07.129

ELSEVIER

Chemical Engineering Science 60 (2005) 467–479

Chemical Engineering Science

www.elsevier.com/locate/ces

Hollow fiber membrane contactor as a gas–liquid model contactor

V.Y. Dindore[a], D.W.F. Brilman[b], G.F. Versteeg[a,*]

[a] *Design and Development of Industrial Processes, Faculty of Chemical Technology, University of Twente, P.O. Box 217, 7500 AE, Enschede, The Netherlands*

[b] *Sasol Technology Netherlands B.V., Hallenweg 5, 7522 NB Enschede, The Netherlands*

Received 30 January 2004; received in revised form 8 July 2004; accepted 27 July 2004
Available online 6 October 2004

Abstract

Microporous hollow fiber gas–liquid membrane contactors have a fixed and well-defined gas–liquid interfacial area. The liquid flow through the hollow fiber is laminar, thus the liquid side hydrodynamics are well known. This allows the accurate calculation of the fiber side physical mass transfer coefficient from first principles. Moreover, in the case of gas–liquid membrane contactor, the gas–liquid exposure time can be varied easily and independently without disturbing the gas–liquid interfacial area. These features of the hollow fiber membrane contactor make it very suitable as a gas–liquid model contactor and offer numerous advantages over the conventional model contactors. The applicability and the limitations of this novel model contactor for the determination of physico-chemical properties of non-reactive and reactive gas–liquid systems are investigated in the present work. Absorption of CO_2 into water and into aqueous NaOH solutions are chosen as model systems to determine the physico-chemical properties for non-reactive and reactive conditions, respectively. The experimental findings for these systems show that a hollow fiber membrane contactor can be used successfully as a model contactor for the determination of various gas–liquid physico-chemical properties. Moreover, since the membrane contactor facilitates indirect contact between the two phases, the application of hollow fiber model contactor can possibly be extended to liquid–liquid systems and/or heterogeneous catalyzed gas–liquid systems.

Keywords: Absorption; Mass transfer; Membranes; Membrane contactor; Model contactor; Multiphase reactors

1. Introduction

A separation or production process using absorption involves transfer of one or more species from the gaseous phase to the liquid phase. In general, the absorption process can be categorized as a physical absorption or a chemical absorption. In the case of physical absorption the gaseous solute is physically dissolved in the liquid phase, whereas in the case of chemical absorption the gaseous solute reacts chemically in the liquid phase. To design an absorption system using either physical or chemical absorption, detailed information is required on the diffusivities and the solubilities of the gaseous solutes in the liquid bulk as well as on the reaction rate kinetics. Various laboratory scale gas–liquid model contactors are used for acquiring this information and for discerning the controlling mechanism in the process of mass transfer accompanied by chemical reactions. In these model contactors the interfacial area is generally known so that the mass transfer coefficient can be calculated from the rate of absorption. The laboratory scale model contactors may be classified into two categories:

(1) Absorbers for which the fluid dynamics of the liquid phase are well understood.
(2) Absorbers which reproduce, on a laboratory scale, the characteristics of industrial absorbers.

The first category includes model contactors like the laminar jet apparatus, the wetted wall column and the rotating drum contactor. In these types of contactors the physical mass transfer coefficient can be estimated theoretically.

* Corresponding author. Tel.: +31-53-489-3327; fax: +31-53-489-4774.
E-mail address: g.f.versteeg@ct.utwente.nl (G.F. Versteeg).

0009-2509/$ - see front matter © 2004 Elsevier Ltd. All rights reserved.
doi:10.1016/j.ces.2004.07.129

Table 1
Comparative evaluation of model contactors

Property	Hollow fiber	Laminar jet	Wetted wall	Stirred cell
G–L exposure time (s)	0.01–10	0.001–0.1	0.1–2	0.06–10
k_L ($m\,s^{-1}$)	1.0×10^{-4}–1.0×10^{-5}	1.6×10^{-3}–1.6×10^{-4}	1.6×10^{-4}–3.6×10^{-5}	1.6×10^{-5}–2.1×10^{-4}
Interface orientation	Orientation free	Vertical	Vertical	Horizontal
Typical liquid use $\times 10^{-6}\,m^3$/expt.	≈ 1000	≈ 5000	≈ 5000	≈ 500
Limitations	Wetting of membrane	Laborious	Laborious	Unknown hydrodynamics
Liquid–Liquid system	Possible	Not possible	Not possible	Possible
Operation mode w.r.t. liquid phase	Continuous	Continuous	Continuous	Batch

The second category includes the disc tower, the multiple-sphere absorber and the stirred cell contactor. In these types of contactors, the physical mass transfer coefficient has to be determined using non-reactive systems. In general, the first category model contactors are used to determine the reaction kinetics and physical properties of gas–liquid system and second category contactors are usually used to simulate the industrial contactors. The details on these types of contactors are given in the literature (Danckwerts, 1970). A comparative evaluation of these types of contactors in terms of achievable contact time and mass transfer coefficients is given in Table 1.

Membrane gas–liquid contactors have a fixed and known mass transfer area, i.e. the physical area of the membrane (Kreulen et al., 1993). This feature of membrane contactors allows easy adaptation of membrane contactors into gas–liquid model contactors to determine the reaction kinetics and physical properties of the gas–liquid system as well as to simulate the industrial absorbers. For example, a flat sheet microporous membrane can be used in the stirred cell to fix the gas liquid interface. This allows use of higher stirring speeds in the liquid phase without disturbing the interfacial area, thus widening the operating range of the stirred cell contactor. Microporous hollow fiber membrane modules can also be conveniently converted into a model contactor. The operation of such a hollow fiber model contactor closely resembles to that of the laminar jet apparatus. The optimized hollow fiber membrane model contactor offers several advantages over the conventional model contactors. Since the liquid flow through the hollow fiber is usually laminar, the liquid side hydrodynamics are well known. This allows the accurate calculation of the physical mass transfer coefficient from first principles. In the case of conventional model contactors in which liquid phase is in continuous mode, e.g. laminar jet and wetted wall column, the entrance and the exit effects affect the determination of the flow patterns and the exact mass transfer area. This limitation is easily eliminated in the hollow fiber membrane model contactor by providing sufficient entrance length for laminar velocity profile to develop before exposing the liquid to the gaseous solute. In the case of the stirred cell apparatus, convection current set near the gas–liquid interface due to temperature variation or concentration variation (initiated if the saturated solution is denser the pure solvent) results into an unstable system. These convection currents can have significant influence on the measurement of the diffusivities and solubilities. These convection currents can be eliminated using narrow hollow fiber membranes. Versteeg and van Swaaij (1988) has successfully applied the method of absorption of a gas into a liquid contained in a narrow tube to determine the gas diffusivities. Thus the hollow fiber membrane contactor is largely free of hydrodynamic constraints.

In the present study, the general applicability of a hollow fiber membrane contactor as model contactor is explored. Initially, physical absorption of carbon dioxide into water was carried out to study the performance of the system at shorter contact times and to optimize the system. Absorption of carbon dioxide into aqueous sodium hydroxide was chosen as a model system to test the applicability for the measurement of chemical and physical parameters for reactive systems.

2. Theory

The rate of absorption of a solute 'A' into an absorbing liquid based on first principle is given by the Fick's law:

$$J_A = -D_A \left(\frac{\partial C_A}{\partial x} \right)_{G\text{–}L \text{ interface}}. \quad (1)$$

However, this procedure is not applicable in most of the cases due to the laborious work required to determine the exact concentration gradient near the gas–liquid interface. Hence, a more simple approach of mass transfer coefficient is used:

$$J_A = k_L(C_{A,i} - C_{A,L}). \tag{2}$$

The mass transfer coefficient can be estimated accurately if the exact hydrodynamics near the interface is known. In the case of a liquid flowing through the hollow fiber, the liquid flow is in the laminar region (for $Re < 2100$) region hence the hydrodynamic conditions near the interface are well known and the liquid side mass transfer coefficient can be calculated from the analogy of Leveque's solution for heat transfer (Leveque, 1928).

$$\text{For } Gz < 10, \quad Sh = \frac{k_L d}{D_A} = 3.67. \tag{3}$$

$$\text{For } Gz > 20, \quad Sh = 1.62\left(\frac{V_L d^2}{D_A L}\right)^{1/3} = 1.62(Gz)^{1/3}. \tag{4}$$

Kreulen et al. (1993) presented a fitted correlation that is valid over the intermediate range of Graetz numbers (Gz) (Graetz, 1883).

$$Sh = \sqrt[3]{3.67^3 + 1.62^3 Gz}. \tag{5}$$

In Eq. (2), $C_{A,L}$ is the mixing cup (analogous to average bulk) concentration of 'A' averaged over the length of the hollow fiber. For laminar flow of liquid through a hollow fiber, with a fully developed velocity profile, the mixing cup concentration of 'A' in the liquid, at any axial distance z from the liquid inlet side of the fiber, is given as follows (Kreulen et al., 1993):

$$C_{m,z} = C_{A,i}\left[1 - \exp\left(-\frac{4k_L z}{V_L d}\right)\right]. \tag{6}$$

The average centerline bulk concentration of 'A' ($C_{A,L}$) in the fiber can be obtained from the integration of $C_{m,z}$ over the length of the fiber:

$$C_{A,L} = \frac{C_{A,i}}{L}\left\{L + \frac{V_L d}{4k_L}\left[\exp\left(-\frac{4k_L L}{V_L d}\right) - 1\right]\right\}. \tag{7}$$

The absorption flux over the length of the fiber can be calculated using Eqs. (2) and (7) if the physical properties of the system are known. Conversely, it is also possible to determine the physical properties of the non-reactive systems from experimental measurements of the absorption flux.

In the case of chemical absorption, the absorption flux is enhanced due to chemical reaction and the average absorption flux is given by

$$J_A = Ek_L(C_{A,i} - C_{A,L}). \tag{8}$$

The enhancement factor 'E' describes the effect of chemical reaction on the mass transfer rate. Generally the enhancement factor (E) is defined as the ratio of absorption flux in presence of chemical reaction to the absorption flux in absence of chemical reaction for identical mass transfer driving force. Several approximate solutions to predict the enhancement factor (E), based on the different mass transfer models, are available in the literature and are applicable over a wide range of process conditions with reactions of differing complexity and chemical solute loading. However, all the models assume the presence of a well-mixed liquid bulk adjacent to the mass transfer zone (relatively large compared to the diffusion zone). This may not be the case for the gas absorption into the liquid flowing through a hollow fiber, especially for smaller diameters. In such cases, depending upon the gas–liquid contact time, the mass transfer zone in the liquid phase of the hollow fiber may actually extend up to the axis of the fiber and the centerline concentration may be disturbed. An additional feature in the gas absorption into a liquid flowing in a hollow fiber is the presence of a velocity profile in the liquid side mass transfer zone. Kumar (2002) used a modified approximate solution to predict the enhancement factor for gas absorption with second-order chemical reaction in a liquid flowing through a hollow fiber. The application of the modified approximate solution was limited to relatively high values of Graetz number. However, rigorous numerical solutions are required to determine the enhancement factor at low Graetz numbers and for complex reactions. The measurement of the absorption flux in different absorption regimes and comparing it with the approximate-analytical or numerical solutions allows the determination of the chemical and physical properties for the reactive systems.

3. Numerical model

For the reactive absorption of a gas in a liquid flowing through a microporous hollow fiber, the differential mass balance for any species 'i' present in the liquid phase is given by

$$v_z\frac{\partial C_i}{\partial z} = D_i\left[\frac{1}{r}\frac{\partial}{\partial r}\left(r\frac{\partial C_i}{\partial r}\right)\right] - S_i. \tag{9}$$

In arriving at Eq. (9), the diffusion in axial direction was neglected and axis-symmetry of the hollow fiber was assumed. 'S' is the source term due to the chemical reaction. Since the liquid flow inside the fiber is laminar, the velocity profile in the radial direction is given by

$$v_z = 2V_L\left(1 - \left(\frac{r}{R}\right)^2\right). \tag{10}$$

The system of partial differential Eq. (9) requires initial and boundary conditions in the axial and radial directions respectively

$$\text{at } z = 0; \text{ for all } r; \quad C_i = C_{i,0}. \tag{11}$$

At the centre of the fiber the concentration profile is symmetric which results in the boundary condition Eq. (12):

$$\text{at } r = 0; \text{ for } z > 0; \quad \left(\frac{\partial C_i}{\partial r}\right) = 0. \tag{12}$$

For a non-volatile liquid phase component flowing through the fiber, the boundary condition at the gas–liquid interface is given by Eq. (13):

$$\text{at } r = R; \text{ for } z > 0; \quad \left(\frac{\partial C_i}{\partial r}\right)_{i \neq A} = 0. \tag{13}$$

At the gas–liquid interface, i.e. the membrane or fiber wall mass transfer of the gas phase solute '*A*' to the liquid phase occurs, which is described by Eq. (14):

$$-D_A \left(\frac{\partial C_A}{\partial r}\right) = k_{\text{ext}}(C_{A,G,\text{bulk}} - C_{A,G,i}). \tag{14}$$

The external mass transfer coefficient (k_{ext}) is a lumped parameter comprising of the resistances to mass transport of species '*A*' due to the gas phase and the microporous membrane;

$$\frac{1}{k_{\text{ext}}} = \frac{1}{k_G} + \frac{1}{k_M}. \tag{15}$$

The set of partial differential equations (the number depends on the number of chemical species involved in the reaction scheme) was solved numerically using a technique described by Versteeg et al. (1989). The concentration profile of the absorbed gas '*A*' in the liquid phase was obtained from the solution of the mass balance equations. The local absorption flux of '*A*' along the length of the fiber was subsequently calculated using Fick's law. The average absorption flux '$\langle J_A \rangle$' was obtained from the integration of the local fluxes along the length of the fiber:

$$\langle J_A \rangle = \frac{1}{L}\int_0^L J_A(z)\,\mathrm{d}z. \tag{16}$$

The exact numerical enhancement factor is defined as the ratio of the absorption rate/flux of a gas in the liquid in the presence of a chemical reaction to the absorption rate/flux in the absence of a reaction:

$$E_{\text{num}} = \frac{\langle J_{A,\text{Chem}} \rangle_{\text{num}}}{\langle J_{A,\text{Phys}} \rangle_{\text{num}}}. \tag{17}$$

It should be noted that the definition for the enhancement factor in Eq. (8) traditionally applies to a situation where the driving force (of solute '*A*') for mass transfer is identical in the presence as well as in the absence of a chemical reaction. However, the above conditions may not be satisfied for long gas–liquid contact times in a membrane contactor (or at low Graetz numbers). In these situations, there will be a significant concentration of *A* in the liquid 'bulk' for the case of physical absorption. Nevertheless, this definition will be used to calculate the overall enhancement factor for a membrane contactor.

4. Characterization of hollow fiber model contactor

As discussed in the previous sections, because of well-defined flow pattern and known mass transfer area, the hollow fiber membrane contactor can be used to determine various physico-chemical properties. In this section, the applicability of this new model contactor for the different absorption regimes is analysed. The possibility of using simplified equations under the limiting cases is also explored.

4.1. Physical absorption

In general, diffusion coefficients of gases in inert liquids are obtained by means of the Taylor capillary method or the diaphragm cell method. However, these methods are time consuming and require considerable quantities of the liquid and the gas. A more rapid and reliable determination of the diffusivity of the gas into the solution is possible using the hollow fiber model contactor.

The Graetz number ($V_L d^2/D_A L$) is the ratio of the penetration time of the solute gas to reach the axis of the hollow fiber (from the gas–liquid interface) to the average residence time of the liquid in the fiber. At higher Graetz number, penetration of the solute is very small as compared to the internal radius of the fiber. Hence at high Graetz numbers, the average bulk concentration of the solute in the fiber is very small. Fig. 1 shows the effect of Graetz number on the average bulk concentration for initially unloaded solvent. It can be seen that at Graetz number larger than 1000, the average bulk concentration can be neglected in comparison with the gaseous solute concentration present at the gas–liquid interface. In this case the absorption process corresponds closely to that into a liquid of infinite depth and the Eq. (2) can be modified to Eq. (18):

$$J_A = k_L C_{A,i} = 1.62\left(\frac{V_L}{dL}\right)^{1/3} D^{2/3} C_{A,i}. \tag{18}$$

Hence at higher Graetz numbers, for the case of hollow fiber model contactor, the gas absorption flux is proportional to the parameter ($D^{2/3}C_{A,i}$). A plot of experimentally

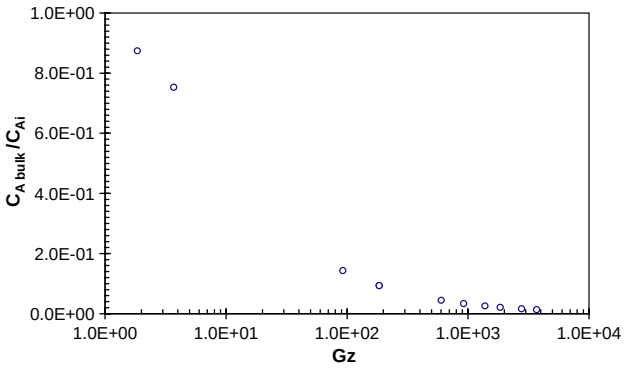

Fig. 1. Effect of Graetz number on the average bulk concentration.

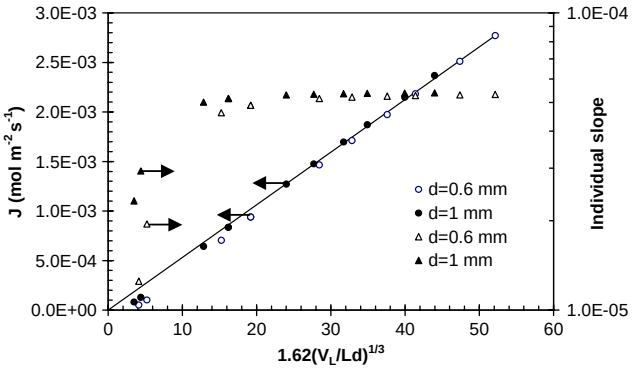

Fig. 2. Estimation of $(D^{2/3}C_{Ai})$ using hollow fiber model contactor. Parameters used: L=0.1 m; C_{AG}=40.87 mol m^{-3}; V_L=1×10^{-3}–2.0 m s^{-1}; $m = 0.845$; $T = 298$ K.

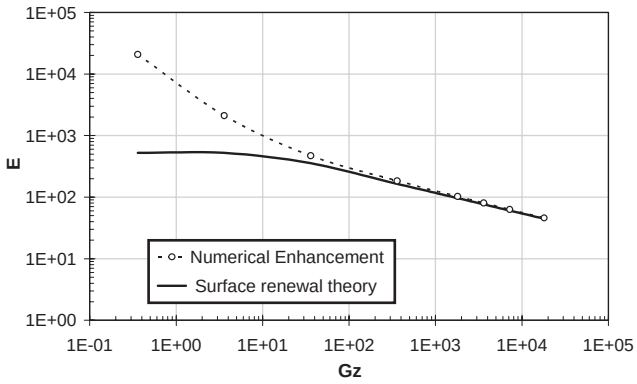

Fig. 3. Effect of Graetz number on the enhancement factor for the gas absorption with first-order irreversible reaction in a liquid flowing through a hollow fiber model contactor. Simulation conditions: $L = 0.1$ m; $d = 600 \times 10^{-6}$ m; $C_{AG} = 10$ mol m^{-3}; $V_L = 1 \times 10^{-4}$–5.0 m s^{-1}; $k_1 = 1000$ s^{-1}; $D_A = 1 \times 10^{-9}$ m^2 s^{-1}; $m = 1.0$. The line indicates the E given by surface renewal theory for first-order irreversible reaction $(E = Ha)$.

measured flux against $1.62(V_L/dL)^{1/3}$ should give a straight line through the origin at high Graetz numbers, having a slope of $(D^{2/3}C_{A,i})$. Thus, at sufficiently high Graetz number $(D^{2/3}C_{A,i})$ can be determined from the slope of the plot using Eq. (18). However, the estimation of the Graetz number requires knowledge about the diffusivity of gas in the solution. Hence the experiments should be carried out at relatively high velocity, small fiber length and larger fiber diameter. A parametric study of the accuracy of this method was done using a theoretical analysis of carbon dioxide absorption into water. A plot of the theoretically calculated flux from Eq. (2) versus the parameter $1.62(V_L/dL)^{1/3}$ is shown in Fig. 2. It can be seen from Fig. 2 that at lower values of $1.62(V_L/dL)^{1/3}$ the data does not follow the straight line correlation through the origin. However, it is possible to draw a straight line passing through the origin for each data point. The slopes of thus drawn individual lines are also plotted in Fig. 2 as a function of $1.62(V_L/dL)^{1/3}$. It can be seen from Fig. 2 that the slopes of these individual lines increases with $1.62(V_L/dL)^{1/3}$ and reaches a plateau at higher values of $1.62(V_L/dL)^{1/3}$. The value of this plateau should be used to calculate $(D^{2/3}C_{A,i})$. Thus if any of the parameter, diffusivity or solubility, is known the other parameter can be determined easily. The comparison between the plots for two different fiber diameters indicates that this plateau is reached at somewhat lower values of $1.62(V_L/dL)^{1/3}$ for larger diameter. This is mainly because as the fiber diameter increases the average bulk concentration in the fiber decreases.

4.2. First-order irreversible reaction

In the case of a first-order irreversible reaction, the local reaction rate is proportional to the concentration of the dissolved gas 'A'. The rate of reaction is given by

$$R_A = -k_1 C_A. \tag{19}$$

Substitution of Eq. (19) in Eq. (9) and solving with the appropriate boundary conditions gives the concentration profile of the solute in the fiber. The average absorption flux and numerical enhancement factor can be calculated using Eqs. (16) and (17), respectively. For mass transfer followed by a first-order irreversible chemical reaction with infinite bulk, the asymptotic approximate solution for the enhancement factor in fast reaction regime ($Ha > 2$) based on surface renewal theory is given by

$$E = Ha, \tag{20}$$

where

$$Ha = \frac{\sqrt{k_1 D_A}}{k_L}. \tag{21}$$

Fig. 3 shows the enhancement factor predicted by the surface renewal theory as well as the exact numerical enhancement factor (Eq. (17)) for reactive absorption of a gas in a liquid flowing at laminar conditions inside the hollow fiber as a function of Graetz number. The enhancement factor based on the surface renewal theory was estimated using mass transfer coefficient, k_L, for the laminar flow conditions in the hollow fiber from Eqs. (3) to (5). It can be seen from Fig. 3 that at higher Graetz numbers, the numerical enhancement E_{num} equals to the enhancement factor predicted by the surface renewal theory. At higher Graetz numbers the average bulk concentration for physical absorption is very small and can be neglected (refer Fig. 1). In this case the driving force for the physical and chemical absorption becomes identical. In addition, the mass transfer zone even for physical absorption is thin and restricted to the gas–liquid interface; therefore the error due to the curvature of the fiber is small and can be neglected. Hence at higher Graetz numbers ($Gz > 1000$), the enhancement factor in the case of gas absorption in a liquid flowing through a hollow fiber can be given by the traditional mass transfer theories and the average absorption flux can be calculated using Eqs. (8) and (20).

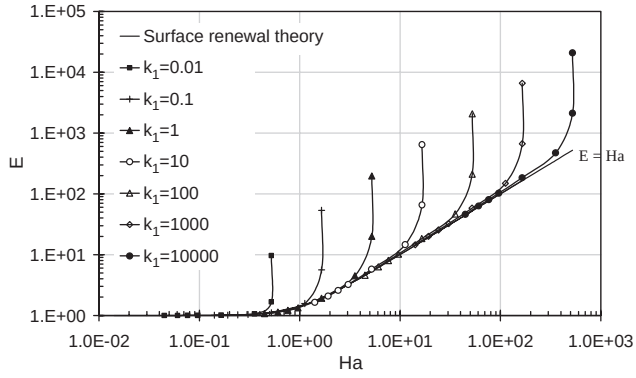

Fig. 4. E versus Ha plot for the gas absorption with first-order irreversible reaction in a liquid flowing through a hollow fiber model contactor. Simulation conditions: $L = 0.1$ m; $d = 600 \times 10^{-6}$ m; $C_{AG} = 10$ mol m^{-3}; $V_L = 1 \times 10^{-4}$–5.0 m s^{-1}; $k_1 = 1 \times 10^{-2}$–1×10^{4} s^{-1}; $D_A = 1 \times 10^{-9}$ m^2 s^{-1}; $m = 1.0$. The line indicates the E given by surface renewal theory for first-order irreversible reaction ($E = Ha$).

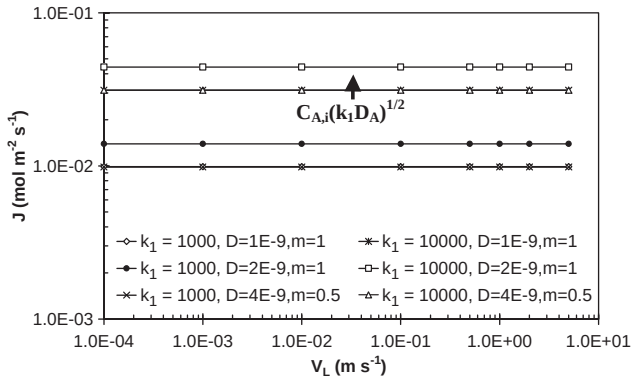

Fig. 5. Effect of liquid velocity on the average absorption flux for the gas absorption in a fast reaction regime in a liquid flowing through a hollow fiber model contactor. Simulation conditions: $L = 0.1$ m; $d = 600 \times 10^{-6}$ m; $C_{AG} = 10$ mol m^{-3}.

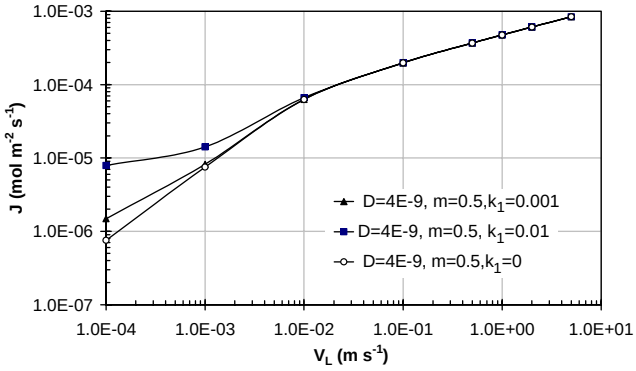

Fig. 6. Effect of liquid velocity on the average absorption flux for the gas absorption in a slow reaction regime in a liquid flowing through a hollow fiber model contactor. Simulation conditions: $L = 0.1$ m; $d = 600 \times 10^{-6}$ m; $C_{AG} = 10$ mol m^{-3}.

In this case the average bulk concentration, C_{AL}, is zero. However, at low values of the Graetz number the numerical enhancement factor is much higher as compared to the enhancement factor predicted by the surface renewal theory. At low Graetz numbers the saturation of the liquid bulk thus substantially reducing the driving force in the corresponding case of physical absorption. In such cases rigorous numerical solutions are required to predict the enhancement factor and hence to calculate the average absorption flux.

In general the enhancement factor due to the chemical reaction is given as the E versus Ha plots. Fig. 4 shows the traditional E versus Ha plot based on approximate solution for the surface renewal theory as well as the exact numerical results for the case of gas absorption in a liquid flowing through a hollow fiber accompanied by first-order reaction. The *Ha*-number was varied by changing the first-order reaction rate constant, k_1, and mass transfer coefficient, k_L (by changing Graetz number). It can be seen from Fig. 4 that there is no unique E–Ha master curve due to the saturation effects in the physical absorption case.

Fig. 5 shows the effect of the liquid velocity and the parameter $C_{A,i}(k_1 D_A)^{1/2}$ on the average absorption flux in the fast reaction regime for different simulation conditions. It can be seen from the figure that the average absorption flux is independent of the liquid velocity and proportional to the parameter $C_{A,i}(k_1 D_A)^{1/2}$. Thus measurements of the experimental absorption flux in this regime, and comparing the measured absorption flux with the flux predicted by traditional mass transfer models using Eqs. (8) and (20) for higher values of Graetz numbers or with the flux predicted using exact numerical simulations, allows the estimation of $C_{A,i}(k_1 D_A)^{1/2}$ group.

In the case of the slow reaction regime, ($Ha < 0.3$), there is no enhancement due to chemical reaction. In this regime the absorption flux depends on the mass transfer coefficient and hence on the liquid velocity. Fig. 6 shows the effect of liquid velocity on the average absorption flux in slow reaction regime. It can be seen from the figure than at higher values of liquid velocities, which corresponds to low Ha number, the chemical absorption flux coincides with the physical absorption flux. In this regime, the absorption flux is again proportional to the parameter $(D^{2/3} C_{A,i})$. Thus by measuring the absorption flux as a function of liquid velocity, the parameter $(D^{2/3} C_{A,i})$ can be estimated.

4.3. Second-order irreversible reaction

In the case of a second-order irreversible reaction, the rate of reaction is proportional to the concentration of the dissolved gas '*A*' as well as the liquid phase reactant '*B*'. The rate of second-order irreversible reaction is given by Eq. (22). The average absorption flux and numerical enhancement factor can be calculated by solving Eq. (9) using Eq. (22):

$$R_A = -k_{1,1} C_A C_B. \tag{22}$$

In the case of mass transfer in a liquid flowing through a hollow fiber accompanied by a second-order (1,1)

irreversible reaction, the saturation of species '*A*' as well as the depletion of species '*B*' in the liquid bulk is important. Under the limiting conditions of high Graetz numbers, the penetration depth of reacting species and hence the reaction zone is confined near the gas–liquid interface. Consequently, liquid far from the interface (at the axis of the fiber) is essentially undisturbed so that the depletion of species '*B*' as well as the saturation of the liquid with the solute can be neglected. This situation is analogous to the situation where a liquid bulk is assumed to be present at infinite distance, as in traditional mass transfer models. At high Graetz numbers the concentration of liquid phase reactant *B* at the axis of fiber is the same as the concentration of *B* at the inlet of the fiber. This situation is also referred as the pseudo-first-order reaction regime. For this case, Kumar (2002) modified the definitions of the dimensionless Hatta number and asymptotic enhancement factor based on the conditions at inlet of the fiber ($z=0$) and showed that, using these definitions it is possible to predict effect of chemical reaction on absorption flux using the approximate asymptotic solutions.

Thus when the Graetz number is relatively high and conditions for the fast reaction regime are satisfied ($2 < Ha \ll E_\infty$), the enhancement factor in the case of hollow fiber model contactor is equal to the modified Hatta number and the average absorption flux can be calculated using Eq. (8) with zero average bulk concentration and the enhancement factor given by Eq. (23). Similar to the irreversible first-order reaction system, in this case also the average absorption flux is independent of k_L (and hence independent of the liquid velocity) and proportional to the parameter $C_{A,i}(k_{1,1}D_A C_{B0})^{1/2}$. Thus from the measurement of experimental absorption flux, the parameter $C_{A,i}(k_{1,1}D_A)^{1/2}$ can be estimated. However, when the depletion of the liquid phase reactant '*B*' is small but not negligible, the rigorous numerical model is required to fit the data:

$$\text{Modified Hatta number}: Ha = \frac{\sqrt{k_{1,1}D_A C_{B,0}}}{k_L}. \tag{23}$$

At low Graetz numbers the penetration depth and hence the reaction zone may extend up to the axis of the fiber. Therefore the absorption regime can continuously change from the liquid entrance to the liquid exit. At the liquid inlet, there is no depletion of the species *B* at the gas–liquid interface and the absorption rate is influenced by the chemical reaction rate (kinetics), while the liquid velocity has no effect on the local absorption rate (Fast regime). Further, along the length of the fiber, depletion of the species '*B*' occurs at the interface. In the case of complete depletion of species '*B*' at the interface, the absorption rate is limited by the radial diffusion of the reacting species to the reaction plane and the flux is strongly influenced by the mass transfer coefficient (Instantaneous regime). At sufficiently low Graetz numbers and when $C_{B0}D_B/C_{A,i}D_A \ll Ha$, the absorption regime over the entire fiber can be assumed as instantaneous reaction regime. In this case, the enhancement factor is given by modified asymptotic infinite enhancement factor and the average absorption flux can be calculated using Eq. (8) with zero average bulk concentration and the enhancement factor given by Eq. (24).

$$\text{Modified infinite enhancement factor}: E_\infty = \left(1 + \frac{C_{B,0}D_B}{\nu_B C_{A,i} D_A}\right)\left(\frac{D_A}{D_B}\right)^n. \tag{24}$$

The value of '*n*' depends on the type of mass transfer model chosen. In the present case where a boundary layer flow is present in the mass transfer zone, hence the value of '*n*' is equal to 1/3. In the instantaneous regime the average absorption flux is determined by C_{Ai}, C_{B0}, D_A, D_B, ν_B and k_L. It may, therefore, be possible to infer the values of one of these quantities from the measure absorption flux if the values of other quantities are known or can be estimated.

For the general case the approximate enhancement factor, based on DeCoursey's solution (using the definition of modified Hatta number and modified infinite enhancement factor), is given by

$$E_{\text{app}} = \frac{-Ha^2}{2(E_\infty - 1)} + \sqrt{\left[\frac{Ha^4}{4(E_\infty - 1)^2} + \frac{E_\infty Ha^2}{(E_\infty - 1)} + 1\right]}. \tag{25}$$

In the extreme case of very low Graetz number, the species '*B*' is completely consumed by the reaction over a certain portion of the fiber and then species '*A*' starts physically absorbing into the liquid phase containing the reaction product till it is saturated with the species '*A*'. In such cases, the enhancement due to the chemical reaction is entirely determined by the stoichiometric coefficients and the concentrations of species '*A*' and '*B*'.

Fig. 7 shows the *E*–*Ha* plot for the case of gas absorption in a liquid flowing through a hollow fiber accompanied by

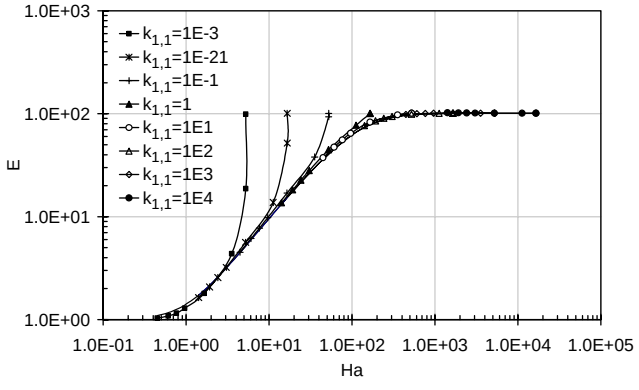

Fig. 7. *E* versus *Ha* plot for the gas absorption with second-order irreversible reaction in a liquid flowing through a hollow fiber model contactor. Simulation conditions: $L=0.1$ m; $d=600\times10^{-6}$ m; $C_{AG}=10$ mol m^{-3}; $C_{B0}=1000$ mol m^{-3}; $V_L=1\times10^{-4}$–5.0 m s^{-1}; $k_1=1\times10^{-2}$–1×10^{4} s^{-1}; $D_B=D_A=1\times10^{-9}$ m^2 s^{-1}; $m=1.0$. The line indicates the *E* given by Decoursey's solution based on surface renewal theory.

a second-order reaction (with $v_B = 1$). By comparing Figs. 7 and 4, it can be seen that the limit (here: 100) is reached in case of second-order reaction for all $k_{1,1}$ values, whereas in case of the first-order reaction no such limit is present.

5. Experimental

Experiments were carried out to explore the applicability of the hollow fiber membrane device as a model contactor for the measurements of physical and chemical parameters. The absorption of carbon dioxide into water was chosen as a model system to measure the physical parameters for a non-reactive system and the absorption of carbon dioxide into aqueous NaOH solutions was chosen as a model system for the measurement of physical and chemical parameter for a reactive system. To measure the combined mass transfer coefficient of the membrane and the gas phase, used in the model development, separate experiments of NH_3 absorption into 2 M sulfuric acid were carried out.

5.1. Selection of process conditions for physical absorption

As discussed in Section 4.1, the simplified method can be used to measure physical parameters with hollow fiber model contactor at relatively high values of Graetz numbers. Hence experiments were carried out at very high Graetz number ($Gz > 1000$) so that the mass transfer zone was confined to the gas–liquid interface and Eq. (18) can be used to predict the average absorption flux. The Graetz number ($V_L d^2/DL$) can be increased by increasing the fiber diameter and/or the liquid velocity through the fiber and by decreasing the fiber length. The higher values of the fiber diameter and the velocity were limited by the critical Reynolds number (2100) for laminar flow. The lower values of the fiber length were limited by the least count of the measurement technique used in the experiments. In view of these limitations, the velocity through the fiber was increased till the Reynolds number remains well below the critical limit. To increase the accuracy of the measurements, instead of a single hollow fiber, a module of five identical short hollow fibers was used. To minimize the gas side mass transfer limitations pure carbon dioxide was used at the shell side of the module. As the hollow fiber model contactor has several advantages over the laminar jet contactor with similar operation, it was tried to achieve the exposure time similar to that are possible with the laminar jet contactor for the possible comparison.

5.2. Selection of process conditions for absorption in fast reaction regime

The absorption of CO_2 in NaOH is followed by a second-order (1,1) irreversible reaction of CO_2 with OH^- ions. At relatively high pH (> 10) values the reaction is given by

$$CO_2 + 2OH^- \rightarrow CO_3^{2-} + H_2O. \quad (26)$$

As discussed in Section 4.2, kinetic parameters can be measured when the reaction occurs in the fast reaction regime over the entire length of the fiber with negligible depletion of OH^- ions. Hence to minimize the depletion of OH^- ions and to carry the reaction in fast absorption regime the following conditions were chosen so that the necessary condition for fast reaction regime $2 < Ha < E_\infty$ is satisfied:

1. A low CO_2 partial pressure was used so as to obtain lower value of $C_{A,i}$.
2. Short exposure time. For this, short fibers with high velocity of the liquid through the fiber were used.
3. Relatively high concentration of OH^- ions was used as an additional effect $C_{A,i}$ also decreases.

The conditions chosen for the measurement of the kinetics are given in Table 2.

5.3. Selection of process conditions for absorption in instantaneous reaction regime

To measure the diffusivity ratio of OH^- ions and carbon dioxide in aqueous NaOH solutions, experiments were carried out in the instantaneous reaction regime. To satisfy the necessary condition ($Ha > E_8$) for the instantaneous reaction regime, experiments were carried out using high partial pressures of CO_2 and long exposure times. Long exposure times were achieved using the low liquid velocities and the long fibers. The experimental conditions chosen for the instantaneous absorption regime are given in Table 2.

5.4. Experimental procedure

Figs. 8a and 8b show schematically the membrane contactor used for the absorption experiments. Microporous polypropylene hollow fibers (Accurel PP: Type Q3/2; average pore diameter: 0.2 μm; inside fiber diameter 600 μm) were used in this study. A module made up of five hollow fibers was used as a model contactor. The five hollow fibers were glued to a liquid distributor with the help of silicon glue. The length of each fiber exposed to the gas was controlled by applying glue on the surface of the membrane. In this way, it was ensured that all five fibers had equal lengths. The glued part of the fiber provides sufficient distance for the laminar liquid flow profile inside the fiber to be fully developed before it contacts the gas. In all the experiments the Reynolds number was maintained well below the critical value for turbulent flow (2100), generally $Re < 1000$.

Fig. 8c shows schematically the experimental setup used for the absorption experiments. A semi-batch mode of gas–liquid contacting operation was used during the experiments. The liquid flow through the fiber was continuous.

Table 2
Experimental conditions

Absorption regime	Fiber length (m)	Velocity ($m\,s^{-1}$)	Graetz number	C_{NaOH} ($mol\,m^{-3}$)	$C_{CO_2,G}$ ($mol\,m^{-3}$)	Temperature (K)
Physical	0.015	0.1–1	1260–12,200	—	48	298
Fast	0.015–0.017	0.8–1	4000–10,100	250–1500	7–8	298–307
Instantaneous	0.017	0.08	800–900	250–1000	52	302

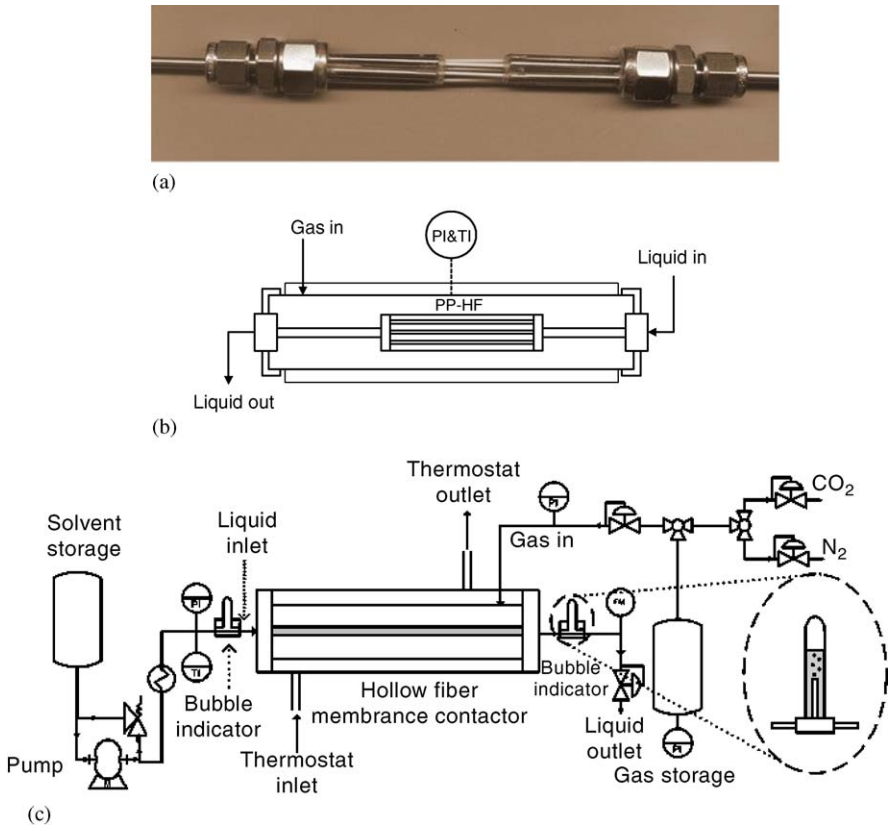

Fig. 8. Hollow fiber membrane model contactor experimental set-up.

The solvent was fed from a high-pressure pump via a flow controller. The solvent used in the experiments was degassed before the usage by applying vacuum in a separate apparatus. Before passing to the hollow fiber module, the solvent was passed through the heat exchanger to maintain the desired temperature. The gas used in the experiments was presaturated with water vapour to ensure that mass transfer was not impeded by the evaporation effects. The carbon dioxide partial pressure outside the hollow fiber in the contactor was maintained constant by feeding pure carbon dioxide from a gas supply vessel, through a pressure regulator. During all the experiments the liquid side pressure was kept sufficiently higher than the shell side gas pressure to avoid the bubbling of gas. From the drop in the pressure of carbon dioxide in the gas supply vessel, the absorption rate and hence the average carbon dioxide flux across the membrane was calculated.

6. Results and discussion

6.1. Measurement of the lumped gas and membrane mass transfer coefficient

The mass transfer coefficient of the membrane phase and the gas phase are combined to give a lumped parameter termed as external mass transfer coefficient k_{ext} in the development of the numerical model. This lumped mass transfer resistance can contribute substantially to the overall mass transfer process when inert are present in the gas phase and/or the enhancement due to the chemical reaction is considerably high. Hence detailed information on the external mass transfer coefficient is important for the accuracy of the data fitting. The membrane mass transfer coefficient can be estimated if the structural properties such as tortuosity (τ) and porosity (ε) of the membrane are known. These

membrane morphological properties are generally determined experimentally. It should be noted that liquids having low surface tension might fill the membrane pores resulting into very low membrane mass transfer coefficient. Hence it is necessary to use more hydrophobic membrane to avoid the wetting of membranes pores in such situations. The estimation of the gas side mass transfer coefficient is rather difficult due to the complex geometry of the contactor and lack of the information on the correlation to predict the gas side mass transfer coefficient for such systems. Hence it was decided to measure the lumped parameter experimentally. The absorption of NH_3 into 2 M sulfuric acid satisfies all criteria for the measurement of gas side mass transfer coefficient (Danckwerts, 1970), hence this system is used to measure the lumped mass transfer coefficient.

In these experiments, first the shell side of the contactor was filled with N_2 to about 110 kPa. A small quantity of NH_3 (8–25 kPa) was added to the shell side. The partial pressure of NH_3 was kept sufficiently small so that evaporation of the water due to the heat of reaction does not result into condensation of water in the module. The average absorption flux was calculated from the mass balance. The lumped mass transfer coefficient was calculated from the experimental absorption flux as given below:

$$k_{\text{ext}} = \frac{J_{\text{expt}}}{C_{G,\text{NH}_3}}. \tag{27}$$

The thus determined value of k_{ext} was $1.01 \times 10^{-2}\,\text{m s}^{-1}$. This estimated value is used for the simulations in the next sections to fit the kinetic and physical parameters.

6.2. Physical absorption experiments

Initial experiments were carried out to optimize the system for high liquid velocity through the fiber and for the short fiber lengths. Fig. 9 shows the plot of k_L versus exposure time. From this figure it can be seen that exposure times in the order of 0.01 s were successfully achieved. The k_L values obtained experimentally are in excellent agreement with those predicted by Leveque's equation with an average deviation of not more than 2%. This result also confirms that the flow within hollow fiber is in the laminar region for these operating conditions.

The absorption of pure carbon dioxide into water was carried out at 298 K to measure the physical parameters. The plot of the experimentally obtained flux versus the parameter $1.62(V_L/dL)^{1/3}$ is shown in Fig. 10. As discussed in Section 4.1, the individual slopes of the line passing through the origin and individual points were also calculated and plotted versus $1.62(V_L/dL)^{1/3}$. The individual slope reaches a constant value of 6.27×10^{-5} at higher values of $1.62(V_L/dL)^{1/3}$. This value of slope was used to calculate the parameter $(D^{2/3}C_{A,i})$. The solubility of the carbon dioxide was taken from the literature (Versteeg and van Swaaij, 1988). From the thus determined values of the parameter

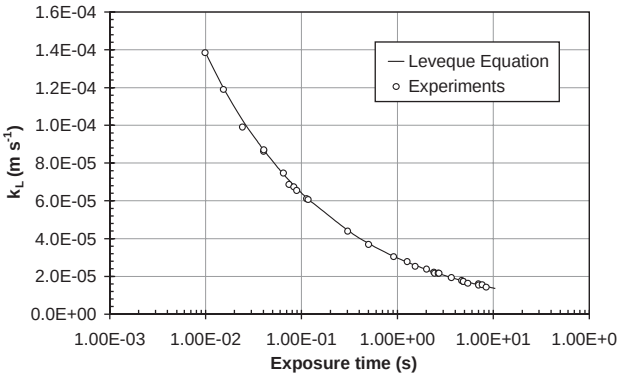

Fig. 9. Liquid side mass transfer coefficient versus exposure time for a hollow fiber model contactor; as determined by CO_2 absorption in water.

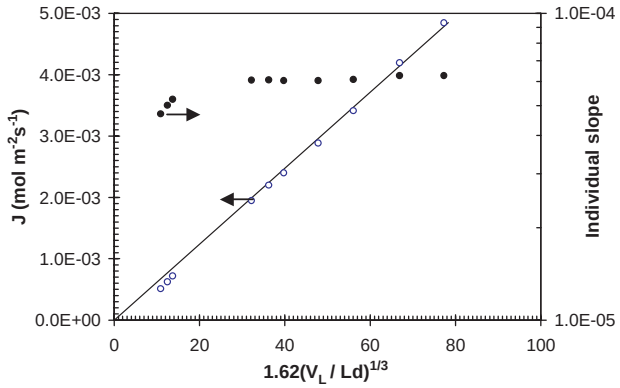

Fig. 10. Estimation of $(D^{2/3}C_{Ai})$ using a hollow fiber model contactor by CO_2 absorption in water. Experiment conditions: $L = 0.015$–0.33 m; $C_{AG} = 48.22\,\text{mol m}^{-3}$; $V_L = 0.05$–$1.0\,\text{m s}^{-1}$; $m = 0.845$; $T = 298$ K.

$(D^{2/3}C_{A,i})$ and the solubility of carbon dioxide, the diffusivity of carbon dioxide into water at 298 K is calculated. This estimated value of the diffusivity ($1.95 \times 10^{-9}\,\text{m}^2\,\text{s}^{-1}$), is in good agreement with the literature reported data ($1.92 \times 10^{-9}\,\text{m}^2\,\text{s}^{-1}$).

6.3. Absorption in fast reaction regime

The surface tension of a NaOH solution is high due to its ionic nature hence the liquid does not wet polyolefin microporous membranes. Considerable and accurate information is available in the literature on the physico-chemical parameters required to model the absorption process. Therefore absorption of CO_2 in aqueous NaOH was used as a model system to the study absorption in different reaction regimes and to check its ability to measure the physical and chemical properties by using a hollow fiber model contactor. In the numerical model reaction Eq. (26) was considered for the simulations. The solubility and diffusivity data used as input parameters in the model were obtained from the literature (Schumpe and Weisenberger, 1996; Hikita et al., 1976). The liquid phase electro-neutrality in the model was

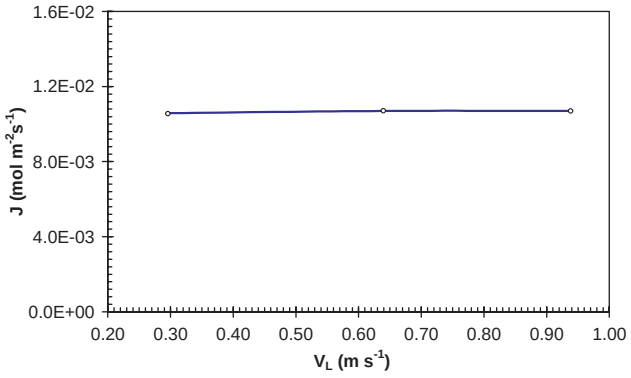

Fig. 11. Effect of liquid velocity on the average absorption flux of CO_2 in 0.5 M NaOH in a hollow fiber model contactor at 303 K.

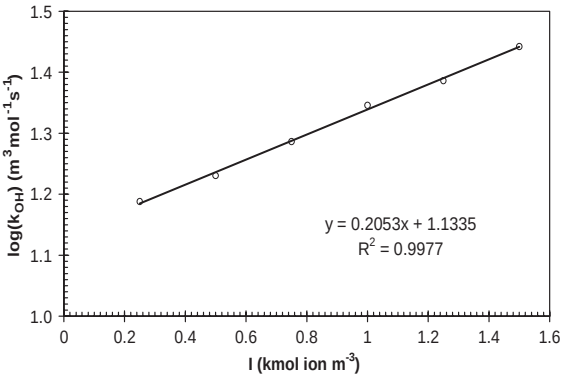

Fig. 13. Effect of ionic strength on the second-order reaction rate constant k_{OH^-} at 307 K.

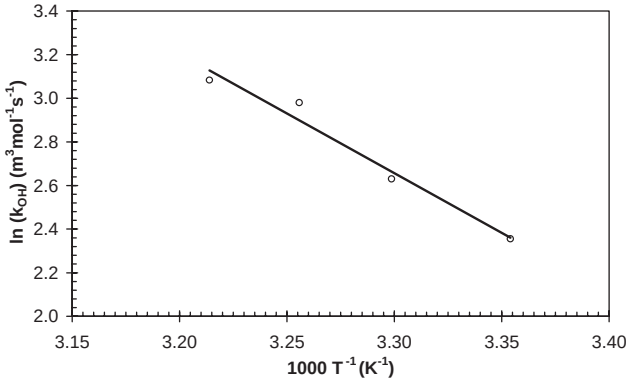

Fig. 12. Arrhenius plot for the second-order reaction rate constant k_{OH^-}.

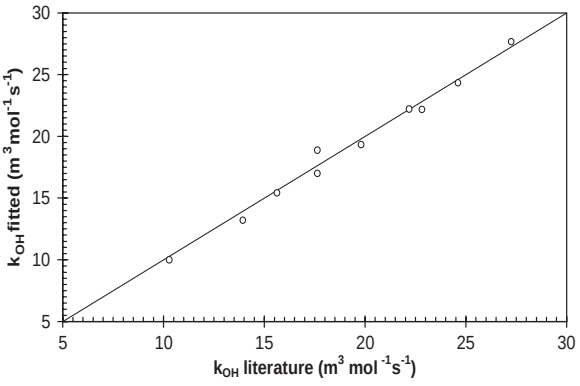

Fig. 14. Parity plot for second-order reaction rate constant k_{OH^-}.

maintained by using mean ion diffusion coefficients for the ionic species in the liquid phase.

To ensure that the absorption takes place in the fast reaction regime the experimental conditions were chosen as discussed in the experimental section. Fig. 11 shows the effect of liquid velocity through the fiber on the average absorption flux. The absorption in the fast reaction regime is confirmed by the fact that flux was found to be independent of the liquid velocity through the fiber. Two different sets of experiments were carried out to study the effect of temperature and to study the effect of ionic strength on the second-order reaction rate constant. To obtain the higher accuracy and to take into account the effect of the lumped external mass transfer coefficient, the numerical model developed in Section 3 was used for the regression of the second-order rate constant.

To estimate the second-order reaction constant of Eq. (26) at various temperature, absorption of CO_2 into 0.5 M NaOH solution was used. Fig. 12 shows the Arrhenius plot for the estimated second-order reaction rate constant for the absorption of CO_2 into 0.5 M NaOH solution. From the Arrhenius plot activation energy 'E_{act}' of the reaction was calculated. The estimated value of the activation energy, 49.3 kJ mol^{-1}, is in good agreement with data reported in the literature, i.e. 44.8 kJ mol^{-1} for the ionic strength of 0.537 kmol m^{-3} (Pohorecki and Moniuk, 1988).

To analyse the effect of ionic strength on the second-order reaction constant of Eq. (26) CO_2 absorption experiments were carried out in NaOH solutions with varying concentrations. Fig. 13 shows the effect of ionic strength on the estimated second-order reaction rate constant at 307 K. It can be seen that in line with the data reported in the literature, the second-order reaction rate constant increases with the ionic strength of the solution. Fig. 14 shows the parity plot for the estimated second-order reaction rate constant and the literature data (Pohorecki and Moniuk, 1988). It can be seen from the figure that there is good agreement between the experimentally estimated second-order reaction rate constant using hollow fiber model contactor and the data reported in the literature.

6.4. Absorption in instantaneous reaction regime

The absorption in the instantaneous regime is governed by the diffusion process of the gaseous solute and the liquid phase reactant. As discussed in Section 4.3, the absorption flux in the instantaneous regime was calculated using Eqs. (8) with zero average bulk concentration and using the

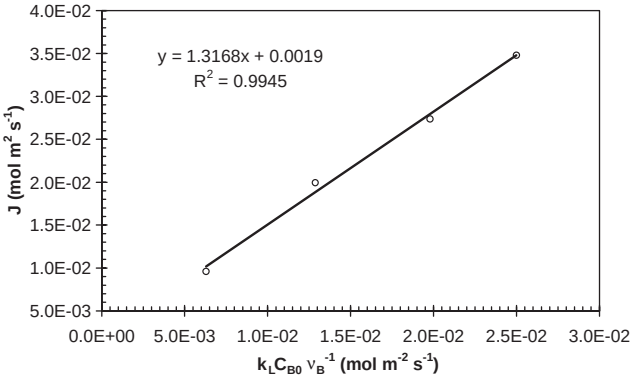

Fig. 15. Average absorption flux versus $k_L C_{B0}/v_B$ for absorption of CO_2 in NaOH in instantaneous regime.

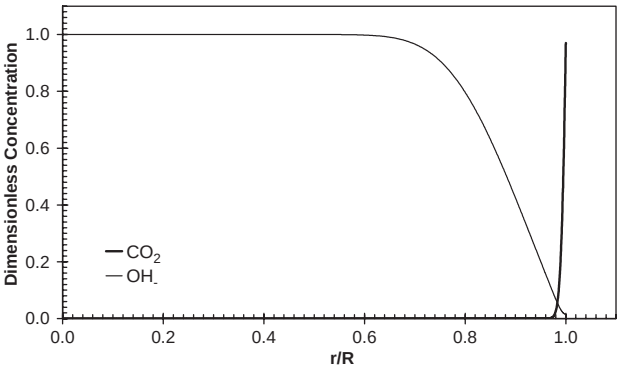

Fig. 16. The calculated radial concentration profile of CO_2 and OH^- ions in the liquid phase.

enhancement factor given by Eq. (24). The flux equation can be simplified as given below:

$$J = k_L\left(\frac{D_A}{D_B}\right)^{1/3} C_{A,i} + \frac{k_L C_{B0}}{v_B}\left(\frac{D_B}{D_A}\right)^{2/3}. \tag{28}$$

The plot of experimentally observed flux versus the parameter $k_L C_{B0}/v_B$ can be used to estimate the diffusivity ratio of the liquid phase reactant to the gaseous solute into the liquid phase. To measure the diffusivity ratio, experiments were carried out in the instantaneous regime at 302 K. To ensure that the absorption take place in the instantaneous reaction regime ($Ha \gg E_\infty$) the experimental conditions were chosen as discussed in the experimental section. The parameter $k_L C_{B0}/v_B$ was varied by changing the concentration of aqueous NaOH solution (i.e. C_{B0}).

Fig. 15 shows the plot of average absorption flux versus $k_L C_{B0}/v_B$. It can be seen from figure that as expected the average absorption flux is proportional to the parameter $k_L C_{B0}/v_B$. The diffusivity ratio can be calculated from the slope of the plot. The value of the ratio of diffusivity of OH^- ions to diffusivity of CO_2 in NaOH solution thus determined is 1.51 and is within 10% of the literature reported value (Nijsing et al., 1959).

When CO_2 reacts with OH^- ions, OH^- disappears and CO_3^{2-} ions are produced in the reaction zone. As a result the diffusion of OH^- to the reaction zone is affected by the counter diffusion of CO_3^{2-}. Although the ionic diffusivity of OH^- ions is higher, the absorption of the CO_2 in instantaneous regime is governed by the effective ionic diffusivity of OH^- ions. Hence the diffusivity ratio obtained and reported in the literature is much lower.

To confirm that the system behaves according to the instantaneous regime, the radial concentration profile of CO_2 and OH^- ions at the liquid exit of the fiber was numerically calculated using the kinetics determined in the previous section and the diffusivity ratio determined in this section. This radial concentration profile for the case of absorption of pure CO_2 into 1 M NaOH at 302 K is shown in Fig. 16. It can be seen from figure that concentration of OH^- ions at the gas–liquid interface reaches to zero and instantaneous absorption regime prevails.

7. Conclusion

In present study, the use of hollow fiber membrane contactors as gas–liquid model contactor for the determination of physical and kinetic parameters for gas–liquid systems is explored. From detailed numerical simulations it was found that at relatively high Graetz numbers (> 1000) the mass transfer zone in the case of gas absorption in a liquid flowing through a hollow fiber is very small and is confined to a region in the vicinity of the gas–liquid interface. In such cases traditional mass transfer theories can be used to describe the mass transfer process with and without chemical reaction. Hence, at relatively high values of the Graetz number, the hollow fiber model contactor can be used to determine physical and chemical properties such as reaction rate constant, diffusivity and solubility from simplified asymptotic solutions. However, for a more complex reaction scheme and at low Graetz numbers a more detailed numerical model is required to fit these parameters.

The effect of unequal driving force, due to the saturation of liquid bulk in the case of physical absorption, in the determination of the enhancement factor for the membrane hollow fiber contactors is recognized and analysed for the cases of first- and second-order reactions.

Experiments were carried out at high Graetz number to estimate the diffusivity and reaction rate constant for known systems namely absorption of CO_2 in water and in NaOH respectively. It was found that the experimentally determined value of the diffusivity of CO_2 in water at 298 K was in excellent agreement with the data reported in the literature. Effect of temperature and ionic strength on the second-order reaction rate constant for the absorption of CO_2 in NaOH was studied using absorption in the fast reaction regime in the hollow fiber model contactor. The second-order reaction rate constant was determined for different temperatures and ionic strengths. The ratio of effective diffusivity of OH^- ions

and diffusivity of CO_2 in liquid phase was determined using absorption in the instantaneous reaction regime in the hollow fiber model contactor. The estimated values of the second-order reaction rate constants and the effective diffusivity ratio were in good agreement with the data reported in the literature.

From the experimental validation it can be concluded that a hollow fiber membrane contactor can successfully be used as a model contactor for the determination of various gas–liquid physico-chemical properties. Moreover, since the membrane contactor facilitates indirect contact between the two phases, the application of hollow fiber model contactor can possibly be extended to liquid–liquid systems and/or heterogeneously catalyzed gas–liquid or liquid–liquid reaction systems.

Notation

C	concentration, mol m^{-3}
D	diffusivity, m^2 s^{-1}
d	diameter, m
E	enhancement factor, dimensionless
Gz	Graetz number, $\frac{vd^2}{Dz}$, dimensionless
Ha	Hatta number, dimensionless
J	flux, mol m^{-2} s^{-1}
k_1	first-order forward reaction rate constant, s^{-1}
$k_{1,1}$	second-order forward reaction rate constant, mol^{-1} m^3 s^{-1}
k	mass transfer coefficient, m s^{-1}
L	length, m
m	distribution coefficient, dimensionless
r	radius, m
Re	Reynolds number, $\frac{dv\rho}{\mu}$, dimensionless
Sh	Sherwood number, $\frac{k_l d}{D}$, dimensionless
V	velocity, m s^{-1}
x	distance, m
z	length, m

Greek letters

ε	porosity, dimensionless
τ	tortuosity, dimensionless
ν	stoichiometric coefficient, dimensionless

Subscripts

G	gas
i	interface; component 'i'
L	liquid
M	membrane
z	local value
0	inletvalue
∞	infinite value

Acknowledgements

This research is part of the research program performed within the Centre for Separation Technology (CST), which is a co-operation between the Netherlands Organization for Applied Scientific Research (TNO) and the University of Twente. We acknowledge Alexey Volkov for his help in experimental work. We would also like to thank Benno Knaken and Wim Leppink for the construction of the experimental set-up.

References

Danckwerts, P.V., 1970. Gas Liquid Reactions, McGraw Hill, New York.

Hikita, H., Asai, S., Takatsuka, T., 1976. Absorption of carbon dioxide into aqueous sodium hydroxide and sodium carbonate and bicarbonate solutions. Chemical Engineering Journal 11, 131–141.

Kreulen, H., Smolders, C.A., Versteeg, G.F., van Swaaij, W.P.M., 1993. Microporous hollow-fiber membrane modules as gas–liquid contactors: 1. Physical mass transfer processes—a specific application: mass transfer in highly viscous liquids. Journal of Membrane Science 78 (3), 197–216.

Kumar, P.S., 2002. Development and design of membrane gas absorption processes. Ph.D. Thesis, University of Twente, The Netherlands.

Leveque, J., 1928. Les lois de la transmission de chaleur par convection. Annls. Mines, Paris (Series 12), 201.

Nijsing, R.A.T.O., Hendriksz, R.H., Kramers, H., 1959. Absorption of CO_2 in jets and falling films of electrolyte solutions, with and without chemical reaction. Chemical Engineering Science 10, 88–104.

Pohorecki, R., Moniuk, W., 1988. Kinetics of the reaction between carbon dioxide and hydroxyl ion in aqueous electrolyte solutions. Chemical Engineering Science 43, 1677–1684.

Schumpe, A., Weisenberger, S., 1996. Estimation of gas solubility in salt solutions at temperatures from 273 K to 363 K. A.I.Ch.E. Journal 42 (1), 298–300.

Stefan, I., 1878. Sitzunsberichte der Akademie der Wissenschaften in Wein 77 (II), 371.

Versteeg, G.F., van Swaaij, W.P.M., 1988. Solubility and diffusivity of acid gases (CO_2, N_2O) in aqueous alkanolamine solutions. Journal of Chemical and Engineering Data 33, 29–34.

Versteeg, G.F., Kuipers, J.A.M., van Beckum, F.P.M., van Swaaij, W.P.M., 1989. Mass transfer with complex reversible chemical reactions. I. Single reversible chemical reaction. Chemical Engineering Science 44, 2295–2310.